

# DEFORMING VIDEOS TO MASKS: FLOW MATCHING FOR REFERRING VIDEO SEGMENTATION

000  
001  
002  
003  
004  
005  
006  
007  
008  
009  
010  
011  
012  
013  
014  
015  
016  
017  
018  
019  
020  
021  
022  
023  
024  
025  
026  
027  
028  
029  
030  
031  
032  
033  
034  
035  
036  
037  
038  
039  
040  
041  
042  
043  
044  
045  
046  
047  
048  
049  
050  
051  
052  
053  
Anonymous authors  
Paper under double-blind review

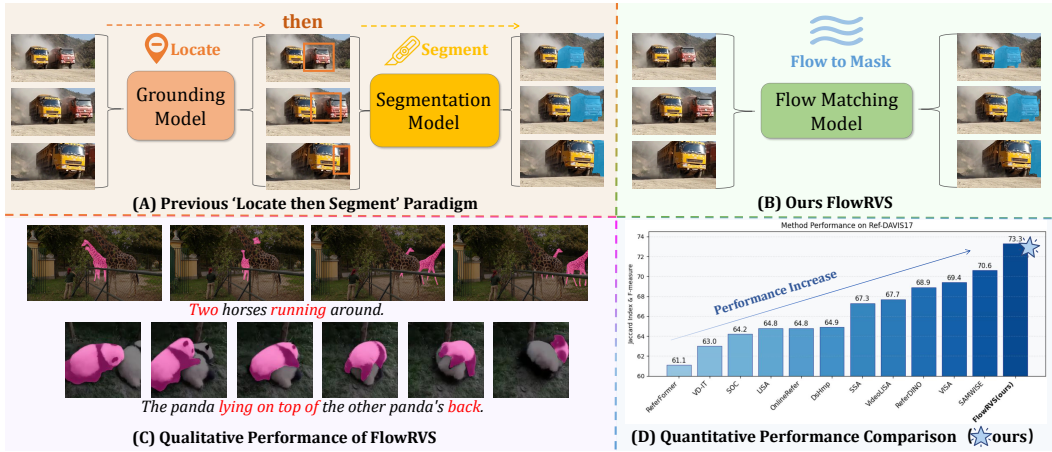


Figure 1: FlowRVS replaces the cascaded ‘locate-then-segment’ paradigm (A) with a unified, end-to-end flow model (B). This new paradigm avoids information bottlenecks, enabling superior handling of complex language and dynamic video (C) and achieving state-of-the-art performance (D).

## ABSTRACT

Referring Video Object Segmentation (RVOS) requires segmenting specific objects in a video guided by a natural language description. The core challenge of RVOS is to anchor abstract linguistic concepts onto a specific set of pixels and continuously segment them through the complex dynamics of a video. Faced with this difficulty, prior work has often decomposed the task into a pragmatic ‘locate-then-segment’ pipeline. However, this cascaded design creates an information bottleneck by simplifying semantics into coarse geometric prompts (e.g, point), and struggles to maintain temporal consistency as the segmenting process is often decoupled from the initial language grounding. To overcome these fundamental limitations, we propose FlowRVS, a novel framework that reconceptualizes RVOS as a conditional continuous flow problem. This allows us to harness the inherent strengths of pretrained T2V models, fine-grained pixel control, text-video semantic alignment, and temporal coherence. Instead of conventional generating from noise to mask or directly predicting mask, we reformulate the task by learning a direct, language-guided deformation from a video’s holistic representation to its target mask. Our one-stage, generative approach achieves new state-of-the-art results across all major RVOS benchmarks. Specifically, achieving a  $\mathcal{J}$ & $\mathcal{F}$  of 51.1 in MeViS (+1.6 over prior SOTA) and 73.3 in the zero shot Ref-DAVIS17 (+2.7), demonstrating the significant potential of modeling video understanding tasks as continuous deformation processes.

## 1 INTRODUCTION

Referring Video Object Segmentation (RVOS) (Khoreva et al., 2018; Gavrilyuk et al., 2018; Hu et al., 2016) requires the machine to segment objects described by natural language queries, which is critical to intelligent systems to precept and interact with the real world (Jiang et al., 2025; Li et al.,

054 2023). The core challenge of RVOS lies in resolving a fundamental spatio-temporal correspondence  
 055 dilemma: anchoring abstract linguistic concepts onto a dynamic and fine-grained pixel space. **Cur-**  
 056 **rent paradigms often rely on instance-centric approaches, which first identify and then track object**  
 057 **instances. While effective, even modern query-based (e.g., ReferFormer (Wu et al., 2022)) or VLM-**  
 058 **based (e.g., LISA (Lai et al., 2024)) methods can introduce an information bottleneck by collapsing**  
 059 **rich semantics into intermediate object-centric representations. This can limit holistic scene under-**  
 060 **standing and temporal consistency, especially as the segmentation of each frame, while conditioned,**  
 061 **doesn't stem from a single, unified spatio-temporal deformation process (Liang et al., 2025b; Ren**  
 062 **et al., 2024; Bai et al., 2024; Lin et al., 2025).**

063 To address these limitations, we argue that pretrained Text-to-Video (T2V) models offer a funda-  
 064 mental solution since their native capabilities for fine-grained, text-to-pixel synthesis and spatio-  
 065 temporal reasoning directly counter the bottlenecks of the ‘locate-then-segment’ paradigm. **While**  
 066 **some attempts use T2V models as powerful frozen feature extractors for a separate decoder (e.g.,**  
 067 **VD-IT (Zhu et al., 2024), HCD (Zhang et al., 2025)), this two-stage design decouples the model’s**  
 068 **generative dynamics from the final task. Our work fundamentally differs: we propose to repurpose**  
 069 **the entire generative process itself, learning a direct, language-guided deformation flow from video**  
 070 **to mask.** DepthFM (Gui et al., 2025) have adapted the entire generative process itself for visual-  
 071 to-visual tasks like depth estimation based on a image generation model. While these pioneering  
 072 efforts validate the generative approach, they also expose a shared, critical blind spot: they fail to  
 073 fully utilize the dynamic, text-driven reasoning that T2V models are capable of and RVOS demands.  
 074 The feature-extraction approach remains decoupled, forcing a separate decoder to reconstruct tem-  
 075 poral relationships from temporally isolated features, squandering the T2V model’s inherent video  
 076 coherence. Meanwhile, the image-to-depth flows proposed by previous styles completely neglect  
 077 text condition, rendering them fundamentally incapable of addressing the core RVOS challenge:  
 078 producing different masks for the same video based on varying textual queries. Thus, we argue that  
 079 a deeper, more principled alignment with the T2V paradigm is required: one that treats the entire  
 080 process as a single, unified, language-guided flow from video pixels to required masks.

081 This unified flow with existing powerful T2V pretrain model (e.g, Wan) brings several benefits: (1)  
 082 their pixel-level synthesis training provides fine-grained control, which enables them to distinguish  
 083 and handle more delicate objects when locating specific targets; (2) their text-condition generation  
 084 ensures powerful multi-modal alignment, which allows them to ground rich linguistic semantics  
 085 directly in the pixel space without as much information loss as first mapping in coarse geomet-  
 086 ric intermediaries; (3) their video-native architecture provides inherent spatio-temporal reasoning,  
 087 naturally unifying language guidance with temporal consistency.

088 However, simply leveraging the T2V framework is not enough. As shown in Figure 3, standard  
 089 T2V generation is a divergent process: it maps a simple noise prior to a set of possible videos,  
 090 exploring a broad trajectory space. RVOS, conversely, is a convergent task: it must map a complex,  
 091 high-entropy video to a single, low-entropy mask. This transforms the problem into a deterministic,  
 092 guided information contraction, where the text query acts as the crucial selector that isolates the  
 093 precise target from the rich visual input (e.g., distinguishing “the smaller monkey” from “the bigger  
 094 monkey”). This core insight that RVOS is a convergent flow directly informs our contributions. To  
 095 successfully manage this asymmetric transformation, we introduce a suite of principled adaptations:  
 096 (1) a boundary-biased sampling strategy to force the model to master the crucial, high-certainty start  
 097 of the trajectory where the video’s influence is strongest; (2) a direct video injection mechanism  
 098 to preserve the rich source context throughout the contraction process; and (3) a task-specific VAE  
 099 adaptation and start point augmentation to create a stable latent space for this unique mapping.

Summarizing, our contributions are as follows:

- 100 • We reformulate RVOS as learning a continuous, text-conditioned flow that deforms a video’s  
 101 spatio-temporal representation into its target mask, directly resolving the correspondence be-  
 102 tween language and dynamic visual data.
- 103 • We propose a suite of principled techniques that successfully enable the transfer of powerful  
 104 text-to-video generative models to this challenging video understanding task.
- 105 • Our proposed framework, FlowRVS, establishes a new state of the art on key benchmarks. No-  
 106 tably, it achieves a significant improvement of **1.6%  $\mathcal{J}$ & $\mathcal{F}$**  on the challenging MeViS dataset  
 107 and **2.7%  $\mathcal{J}$ & $\mathcal{F}$**  on the zero-shot DAVIS 2017 benchmark.

108 

## 2 RELATED WORK

110 **Referring Video Object Segmentation** aims to segment a target object within a video based on a  
 111 natural language expression (Xu et al., 2018; Ding et al., 2023). This task demands both visual-  
 112 linguistic understanding and robust temporal segmenting. Early approaches often adapted frame-  
 113 level referring image segmentation models and appended temporal linking mechanisms as a post-  
 114 processing step (Khoreva et al., 2018). More recent and competitive methods have evolved into  
 115 more integrated yet predominantly multi-stage pipelines. A dominant paradigm involves a “locate-  
 116 then-segment” strategy, where a powerful multi-modal model first grounds the textual reference to a  
 117 spatial region, which then guides a separate segmentation process for each frame.

118 **“Locate-then-Segment” Paradigm** manifests in several forms. A significant breakthrough came  
 119 with the introduction of query-based architectures, inspired by the success of DETR-style (Zhu et al.,  
 120 2020) transformers in vision tasks (Wu et al., 2022; Yan et al., 2024b), this new paradigm reframed  
 121 RVOS by treating language as a query to the visual features. Furthermore, multimodal model based  
 122 approaches like LISA (Lai et al., 2024), VISA (Yan et al., 2024a) and ReferDINO (Liang et al.,  
 123 2025b;a) leverage a pretrained model’s reasoning or grounding ability, such as LLaVA(Liu et al.,  
 124 2023) or DETR-based GroundingDINO (Ren et al., 2024), to perform initial object localization, and  
 125 then introduce a custom-designed mask decoder to generate the final segmentation. A similar phi-  
 126 losophy is seen in the “VLM+SAM” family of methods (Luo et al., 2023; Wu et al., 2023), which  
 127 use a Vision-Language Model for bounding box prediction, followed by a generic segmentation  
 128 model like SAM (Kirillov et al., 2023; Cuttano et al., 2025) to produce pixel-level masks (He &  
 129 Ding, 2024; Lin et al., 2025; Pan et al., 2025). Another line of work explores repurposing generative  
 130 models: VD-IT (Zhu et al., 2024) first extracts features from a pretrained text-to-video diffusion  
 131 model and then feeds these features into a separate DETR-like architecture for mask prediction.  
 132 While these methods have pushed the performance boundaries, their reliance on intermediate rep-  
 133 resentations—whether object queries or extracted features—can introduce information bottlenecks  
 134 that prevent a truly holistic, end-to-end optimization of the video-to-mask correspondence problem.

135 **Generative Modeling** is largely catalyzed by the advent of latent diffusion models (Rombach et al.,  
 136 2022). Building on this success, the frontier rapidly expanded into the temporal domain, leading to  
 137 a surge of powerful text-to-video (T2V) models (Liu et al., 2024; Wan et al., 2025; Gao et al., 2025).  
 138 Recent works have begun to leverage these models for RVOS. A notable approach (e.g., VD-IT (Zhu  
 139 et al., 2024), HCD (Zhang et al., 2025)) utilizes T2V models as powerful frozen feature extractors for  
 140 a separate segmentation decoder. Our work fundamentally differs: instead of extracting features, we  
 141 repurpose the entire generative process, fine-tuning the core model to learn a direct video-to-mask  
 142 deformation flow. This avoids the bottleneck inherent in a two-stage pipeline. Furthermore, unlike  
 143 conditional generation frameworks like ControlNet(Zhang et al., 2023) that add external guidance to  
 144 a divergent, noise-to-image process, our method learns a convergent, discriminative transformation  
 145 from the video source itself. Beyond diffusion, Flow Matching (Lipman et al., 2022; Liu et al.,  
 146 2022) offers a significant theoretical advancement by learning a velocity field to transport samples  
 147 along a deterministic ODE path. This has been leveraged for visual tasks like depth estimation  
 148 (e.g., DepthFM (Gui et al., 2025)), but these methods are typically text-agnostic. Our work makes  
 149 a critical distinction: we introduce the natural language query as the core conditional force that  
 150 modulates the entire ODE path. This elevates the framework from a simple translation to a dynamic,  
 151 multi-modal reasoning engine, reframing RVOS as a learned, conditional deformation.

152 

## 3 METHOD

153 

### 3.1 PROBLEM REFORMULATION: RVOS AS A CONTINUOUS FLOW

154 Traditionally, RVOS is approached as a discriminative, one-step prediction task. A model  $f_\theta$  is  
 155 trained to learn a direct mapping  $M = f_\theta(V, c)$  from a video-text pair to a mask sequence. How-  
 156 ever, this direct mapping is fundamentally challenged by the need to collapse a dynamic, high-  
 157 dimensional video into a precise pixel-mask under the complex constraints of a linguistic instruction,  
 158 all within a single transformation.

159 To overcome this limitation, we depart from direct prediction and reconceptualize RVOS as a **text-  
 160 conditioned continuous flow problem**. We propose to model segmentation as a gradual, determin-  
 161 istic deformation process that transforms the video’s representation into the target mask’s. This is

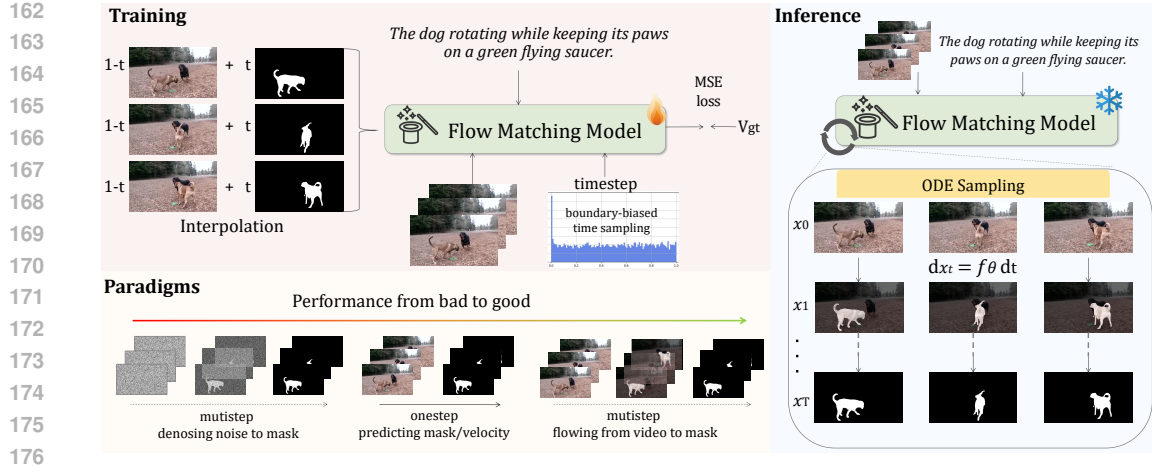


Figure 2: FlowRVS reformulates RVOS as a text-conditioned continuous flow, learning a velocity field via Flow Matching stabilized by boundary-biased time sampling in latent space. During inference, an ODE solver uses this field to deterministically deform the video latent to the target mask, this video to mask paradigm superior to noise-based or one-step prediction approaches.

governed by an Ordinary Differential Equation (ODE), where our goal is to learn the velocity field  $\mathbf{v}(\mathbf{z}_t, c, t)$  that dictates the evolution of a latent state  $\mathbf{z}_t$ :

$$\frac{d\mathbf{z}_t}{dt} = \mathbf{v}(\mathbf{z}_t, c, t), \quad \text{with boundary conditions } \mathbf{z}_0 \sim \mathcal{P}_{\text{video}} \text{ and } \mathbf{z}_1 \sim \mathcal{P}_{\text{mask}}. \quad (1)$$

The trajectory starts from the video latent  $\mathbf{z}_0$  and is guided by the text query  $c$  to terminate at the specific mask latent  $\mathbf{z}_1$ . This transforms the learning objective from mastering a single, complex global function to learning a simpler, local velocity field.

However, adapting this generative-native paradigm to a discriminative task like RVOS is not straightforward, but a fundamental inversion of the generative process, as illustrated in Figure 3. Standard T2V generation is a divergent, one-to-many process: it starts from a simple, fixed noise distribution and has a broader exploration space in the initial steps to generate a diverse set of plausible videos. In contrast, our approach is a convergent, video-text-to-one task. It begins with a complex, high-entropy video latent  $\mathbf{z}_0$  and must follow a more tightly mapped direction to a single, correct mask. Here, the text query  $c$  is no longer a creative prompt but a critical, disambiguating force. The initial velocity computed from  $\mathbf{z}_0$  must be precise enough to distinguish “the smaller monkey” from “the bigger monkey.” An error in this first step is irrecoverable, dooming the entire trajectory to fail. This places paramount importance on correctly learning the starting point of the flow.

### 3.2 TRANSFERRING TEXT-TO-VIDEO MODEL TO RVOS

A naive, uniform treatment of the trajectory, inherited from generative modeling, fails to account for the unique asymmetric nature of the video-to-mask flow. This asymmetry—a high-certainty, structured start and a low-certainty, sparse end—demands a non-uniform approach to learning the velocity field. Therefore, we introduce a suite of three synergistic strategies grounded in a single principle: fortifying the flow’s origin. These are designed not as independent tweaks, but as a cohesive framework to successfully adapt the powerful T2V model for RVOS.

**Boundary-Biased Sampling (BBS).** We hypothesize that the most critical learning signal resides at the beginning of the trajectory, where the model computes the initial “push” away from the video manifold based on the text query. To exploit this, we introduce BBS, a curriculum learning strategy that oversamples timestep  $t = 0$ . By concentrating the gradient updates on this initial, high-influence decision, we force the model to first master the crucial text-guided velocity computation. As empirically demonstrated in Table 2, this focused learning strategy is the key to stabilizing the training process, transforming the failing baseline into a highly effective model by ensuring a well-posed initial value problem for the ODE.

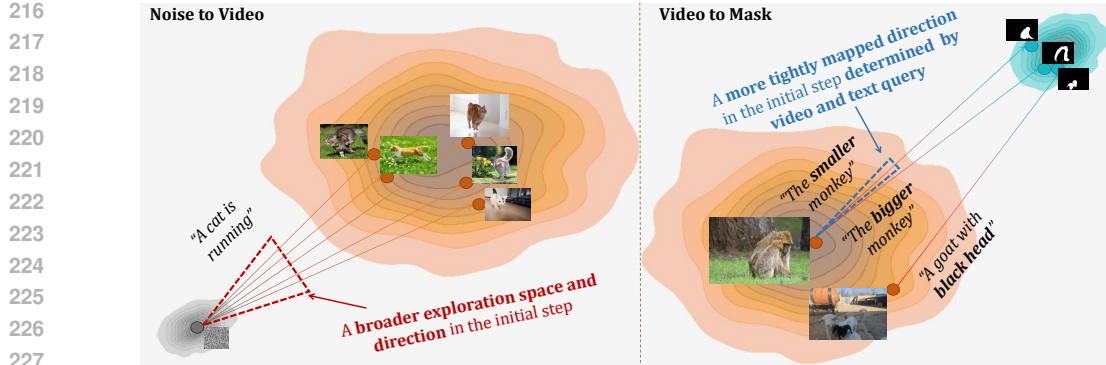


Figure 3: Repurposing a generative process for a discriminative task. Unlike standard T2V generation which maps noise to diverse videos (left), our method maps a complex video to a single mask (right). This transforms the process into a deterministic, convergent task where the text query is the crucial element that selects the precise target from the visual input (e.g., distinguishing the ‘smaller’ from the ‘bigger’ monkey).

**Start-Point Augmentation (SPA).** To prevent the model from overfitting to discrete points on the data manifold and to encourage the learning of a smoother, more generalizable flow, we introduce Start-Point Augmentation (SPA). During training, we transform the initial video latent  $\mathbf{z}_0$  through a stochastic encoding and normalization process. This technique effectively presents the model with a richer, locally continuous distribution of starting points centered around the original video latent. This acts as a powerful regularizer, forcing the model to learn a velocity field that is robust not just on the manifold, but also in its immediate vicinity.

**Direct Video Injection (DVI).** In our video-to-mask formulation, the initial video latent  $\mathbf{z}_0$  is not merely a starting point, but the foundational context for the entire transformation. To ensure this context remains accessible throughout the flow, we introduce Direct Video Injection (DVI). We implement this by concatenating the original video latent  $\mathbf{z}_0$  with the current state  $\mathbf{z}_t$  along the channel dimension at each ODE step without introducing heavy computational burden. This transforms the velocity prediction at every subsequent point from  $v(\mathbf{z}_t, t)$  to  $v([\mathbf{z}_t, \mathbf{z}_0], t)$ , explicitly conditioning each local update on the global origin. This simple yet effective strategy provides a persistent, high-fidelity reference to the source video, preventing trajectory drift and improving fine-grained accuracy with negligible computational overhead.

### 3.3 ANALYSIS OF ALTERNATIVE PARADIGMS

To motivate our final choices, we first analyze the fundamental limitations of three plausible alternative paradigms for adapting a T2V model to RVOS. As empirically validated in our ablation studies, each of these alternatives fails due to a core mismatch with the nature of RVOS. **To ensure a fair comparison, all alternative paradigms were built upon the same Wan2.1 pre-trained model and trained under the exact same supervised setting (same optimizer, learning rate, and duration) as our final model. And we implemented the same fine-tuned VAE to reveal the superiority of our proposed flow-based paradigm.**

**Direct Mask Prediction (Worst Performance).** A direct, single-step mapping from the video and text latents to the mask latent represents the classic discriminative paradigm. We argue this approach is fundamentally ill-posed due to what we term “information collapse.” The mapping from a high-entropy, complex video manifold to a low-entropy, sparse mask manifold is a drastic information contraction. Forcing a neural network to learn this in a single, abrupt step leads to collapse of the rich visual context into a coarse approximation rather than performing a precise, guided refinement. The model is not learning a transformation, but rather a brittle pattern recognition function.

**Noise-to-Mask Flow (Suboptimal).** This paradigm mirrors standard text-to-video generation, starting from Gaussian noise  $\mathbf{z}_1 \sim \mathcal{N}(0, I)$  and conditioning on the video context. This approach

270 demotes the video from the primary source of information to a secondary condition. Weaken the  
 271 guidance of the video in the process would possibly force the entire, high-dimensional video context  
 272 to be injected via a simple concatenation at each step, creating a severe information bottleneck. The  
 273 model is tasked with generating the mask’s complex spatio-temporal structure from scratch based  
 274 on this limited conditional signal, rather than progressively refining the rich, structured information  
 275 already present in the video itself.

277 **One-Step Velocity Prediction (Better, but Limited).** This paradigm makes the model predict the full  
 278 velocity vector  $\mathbf{v} = \mathbf{z}_1 - \mathbf{z}_0$  in a single inference step. It significantly outperforms the previous  
 279 two baselines, confirming our hypothesis that learning a residual velocity is a more stable and ef-  
 280 fective objective than predicting an absolute state. However, its performance is still fundamentally  
 281 capped. We assume that it is limited by the need to compute the entire, often large-magnitude de-  
 282 formation in a single forward pass, lacking the capacity for the gradual, iterative refinements that a  
 283 multi-step process allows.

284 This analysis solidifies our central thesis: a multi-step, video-to-mask flow is the most effective  
 285 paradigm for RVOS, but only when augmented with our proposed start-point focused adaptations to  
 286 bridge the critical gap between its generative origins and the discriminative demands of the task.

## 288 4 EXPERIMENTS

### 291 4.1 BENCHMARK AND METRICS

293 We evaluate our framework on three standard RVOS benchmarks. MeViS (Ding et al., 2023) is a  
 294 challenging, motion-centric benchmark featuring 2,006 long videos and over 28,000 fine-grained  
 295 annotations that emphasize complex dynamics. Ref-YouTube-VOS (Wu et al., 2022) is the large-  
 296 scale benchmark, comprising 3,978 videos that test for generalizability across a wide diversity of  
 297 objects and scenes. Ref-DAVIS17 (Khoreva et al., 2018) is a high-quality, densely annotated dataset  
 298 of 90 videos, serving as a key benchmark for segmentation precision and temporal consistency.

299 Following standard protocols, we report region similarity ( $\mathcal{J}$ , Jaccard Index), contour accuracy ( $\mathcal{F}$ ,  
 300 F-measure), and their average ( $\mathcal{J} \& \mathcal{F}$ ) as our primary evaluation metrics.

### 302 4.2 IMPLEMENTATION DETAILS

304 Our framework is built upon the publicly available Wan 2.1 text-to-video model, which features a  
 305 1.3B parameter Diffusion Transformer (DiT) (Wan et al., 2025). Throughout all training stages, we  
 306 keep the pretrained text encoder and the VAE encoder entirely frozen. Our training focuses exclu-  
 307 sively on fine-tuning the DiT block to learn the conditional flow. Crucially, the VAE decoder is  
 308 specifically adapted for the segmentation task by being fine-tuned separately on the MeViS training  
 309 set, allowing it to specialize in reconstructing high-quality masks from the latent space. [Our training  
 310 protocol varies by dataset to align with the same evaluation protocols of compared methods.](#)  
 311 For experiments on Ref-YouTube-VOS, we follow a two-stage training strategy. The model is first  
 312 pre-trained on a combination of static image datasets (RefCOCO/+g) (Yu et al., 2016; Kazemzadeh  
 313 et al., 2014) to learn foundational visual-linguistic grounding. Subsequently, this pre-trained model  
 314 is fine-tuned on the Ref-YouTube-VOS training set. The final weights from this stage are then  
 315 used for zero-shot evaluation on the Ref-DAVIS17 benchmark without any further fine-tuning to  
 316 prove FlowRVS’s generalization ability. For the more challenging MeViS dataset, which empha-  
 317 sizes complex motion understanding, we train our model directly on its training set from scratch,  
 318 without leveraging any static image pre-training. More hyperparameters settings can be found in  
 319 Appendix A.

### 320 4.3 MAIN RESULTS

322 We compare our proposed FlowRVS against a wide range of baselines in Table 1. Our results show  
 323 that FlowRVS significantly and consistently outperforms previous approaches. We highlight some  
 324 key features as follows:

324  
 325 Table 1: Comparison of our one-stage FlowRVS with other previous ‘locate-then-segment’ methods  
 326 on MeViS, Ref-YouTube-VOS and Ref-DAVIS datasets. We further include methods based on large  
 327 VLMs for comparison. **Bold** and underline indicate the two top results.

328 Method	329 MeViS			330 Ref-YouTube-VOS			331 Ref-DAVIS17		
	$\mathcal{J}\&\mathcal{F}$	$\mathcal{J}$	$\mathcal{F}$	$\mathcal{J}\&\mathcal{F}$	$\mathcal{J}$	$\mathcal{F}$	$\mathcal{J}\&\mathcal{F}$	$\mathcal{J}$	$\mathcal{F}$
<i>332 Locate-then-segment</i>									
333 MTTR [CVPR’22]	30.0	28.8	31.2	55.3	54.0	56.6	-	-	-
334 ReferFormer [CVPR’22]	31.0	29.8	32.2	62.9	61.3	64.6	61.1	58.1	64.1
335 SOC [NIPS’23]	-	-	-	66.0	64.1	67.9	64.2	61.0	67.4
336 OnlineRefer [ICCV’23]	32.3	31.5	33.1	63.5	61.6	65.5	64.8	61.6	67.7
337 LISA [CVPR’24]	37.2	35.1	39.4	53.9	53.4	54.3	64.8	62.2	67.3
338 DsHmp [CVPR’24]	46.4	43.0	49.8	67.1	65.0	69.1	64.9	61.7	68.1
339 VideoLISA [NIPS’24]	42.3	39.4	45.2	61.7	60.2	63.3	67.7	63.8	71.5
340 VD-IT [ECCV’24]	-	-	-	64.8	63.1	66.6	63.0	59.9	66.1
341 VISA [ECCV’24]	43.5	40.7	46.3	61.5	59.8	63.2	69.4	66.3	72.5
342 SSA [CVPR’25]	48.9	44.3	53.4	64.3	62.2	66.4	67.3	64.0	70.7
343 SAMWISE [CVPR’25]	<b>49.5</b>	<b>46.6</b>	52.4	69.2	<b>67.8</b>	70.6	<b>70.6</b>	<b>67.4</b>	<b>74.5</b>
344 ReferDINO [ICCV25]	49.3	44.7	<u>53.9</u>	<u>69.3</u>	67.0	<u>71.5</u>	68.9	65.1	72.9
<i>345 One-stage generation based</i>									
346 <b>FlowRVS (ours)</b>	<b>51.1</b>	<b>47.6</b>	<b>54.6</b>	<b>69.6</b>	<u>67.1</u>	<b>72.1</b>	<b>73.3</b>	<b>68.4</b>	<b>78.2</b>

347  
 348  
 349 **Dominance on Complex Motion-Centric Benchmarks.** The most significant advantage of our  
 350 framework is demonstrated on MeViS, the most challenging benchmark designed to test a nuanced  
 351 understanding of motion-centric language. FlowRVS achieves a  $\mathcal{J}\&\mathcal{F}$  score of 50.7, establishing a  
 352 new SOTA and surpassing the previous best method, SAMWISE, by a substantial 1.2 point margin.  
 353 This result is particularly noteworthy as MeViS features long videos with complex object interac-  
 354 tions and appearance changes—scenarios where the limitations of multi-stage, cascaded pipelines  
 355 are most exposed. The superior performance of FlowRVS directly validates our core thesis: a holis-  
 356 tic, end-to-end flow that models the entire video-to-mask transformation is fundamentally better  
 357 suited to capture and reason about complex spatio-temporal dynamics.

358 **Superiority over ‘Locate-then-Segment’ Paradigms.** Our performance gains are particularly  
 359 meaningful when compared directly against methods that epitomize the ‘locate-then-segment’  
 360 paradigm, such as VISA (VLM-based) and ReferDINO (grounding-model-based). On MeViS,  
 361 FlowRVS outperforms VISA-13B by a remarkable 7.0 points and ReferDINO (best results an-  
 362 nounced in the paper) by 1.4 points. This underscores the advantage of our one-stage approach.  
 363 By avoiding the irreversible information loss inherent in collapsing semantics into an interme-  
 364 diate geometric or feature prompt, our continuous flow process maintains a high-fidelity, text-guided  
 365 transformation from start to finish, leading to more accurate and robust segmentation. The funda-  
 366 mental advantages of our one-stage flow paradigm are further illustrated in our qualitative com-  
 367 parisons (Figure 4). For the query “The white rabbit which is jumping,” ReferDINO provides a coarse,  
 368 static grounding of the rabbit but misses the jumping action’s details, whereas FlowRVS delivers a  
 369 precise, dynamic segmentation. More critically, for the temporal query “The first tiger...”, VD-IT’s  
 370 decoupled decoder fails to resolve the ambiguity and tracks the wrong target. In contrast, FlowRVS  
 correctly identifies and tracks the first tiger throughout, demonstrating superior global reasoning.

371 **Exceptional Zero-Shot Generalization on Ref-DAVIS17.** The generalization capability of our  
 372 model is best illustrated by its zero-shot performance on Ref-DAVIS17. Without any fine-tuning on  
 373 the DAVIS dataset, the model trained on Ref-YouTube-VOS achieves a  $\mathcal{J}\&\mathcal{F}$  score of 73.3. This  
 374 result is not only state-of-the-art but is also significantly higher than many previous methods that  
 375 were explicitly trained or fine-tuned on similar high-quality datasets. This strong zero-shot trans-  
 376 ferability suggests that our flow-based paradigm, by learning a more fundamental and continuous  
 377 mapping between video and its corresponding mask guided by language, develops a more general-  
 378 izable understanding of spatio-temporal correspondence that is less prone to dataset-specific biases.

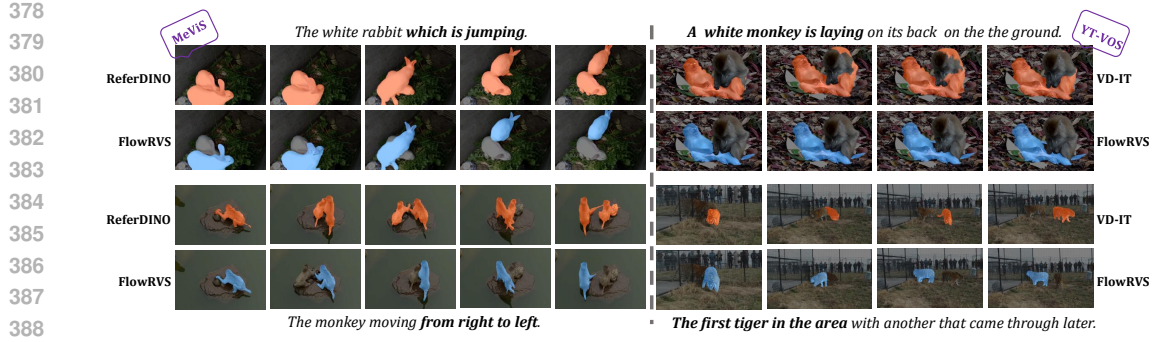


Figure 4: Qualitative comparison on challenging temporal and linguistic reasoning. Prior paradigms struggle: VD-IT produces temporally unstable masks due to its frame-wise decoder, while ReferDINO fails to interpret long-range descriptions. Our method, FlowRVS, demonstrates superior temporal coherence and language grounding by leveraging an end-to-end generative process.

Table 2: Ablations of FlowRVS on the MeViS  $valid_u$  set. BBS: Boundary-Biased Sampling (probability  $p$ ). DVI: Direct Video Injection. SPA: Start Point Augmentation. WI: Weight Init from Wan.

ID	Method Configuration	BBS ( $p$ )	SPA	DVI	WI	$\mathcal{J} \& \mathcal{F}$	$\mathcal{J}$	$\mathcal{F}$
<i>Alternative Paradigms</i>								
(a)	MutiStep Noise-to-Mask Flow	–	–	✓	✓	32.3	29.6	35.0
(b)	Onestep Mask Prediction	–	–	–	✓	36.2	41.5	38.9
(c)	Onestep Velocity Prediction	–	–	–	✓	50.8	47.1	54.4
<i>Our MutiStep Video-to-Mask Flow</i>								
(c)	Base Flow	0.0	–	–	✓	47.9	42.9	52.9
(d)	+ BBS	0.25	–	–	✓	55.2	50.7	59.6
(e)	+ BBS	0.50	–	–	✓	57.9	53.8	62.1
(f)	+ BBS	0.75	–	–	✓	56.5	52.5	60.4
(g)	+ SPA	0.50	✓	–	✓	58.6	54.2	63.0
(h)	+ DVI (ours default)	<b>0.50</b>	✓	✓	✓	<b>60.6</b>	<b>55.9</b>	<b>65.2</b>
(i)	- WI	0.50	✓	✓	✗	21.1	20.3	21.9

#### 4.4 ABLATION STUDIES

We conduct our ablation studies on the challenging MeViS dataset, as its complex, motion-centric scenarios provide a rigorous testbed for our design choices. To ensure a consistent and fair comparison, all results are reported on the  $valid_u$  set, following the protocol in prior work (Ding et al., 2023). The results are summarized in Table 2.

**Analysis of Alternative Paradigms.** Our investigation begins by establishing the limitations of alternative paradigms (rows a-c). The Noise-to-Mask Flow (a), which mirrors standard generative practices, performs poorly (32.3  $\mathcal{J} \& \mathcal{F}$ ). This confirms our hypothesis that demoting the video to a secondary condition (concatenate with noise) creates a severe information bottleneck, forcing the model to generate the mask from scratch. The Onestep Mask Prediction model (b) also struggles (36.2  $\mathcal{J} \& \mathcal{F}$ ), validating that a single, abrupt mapping is insufficient to bridge the vast representational chasm between video and mask. Notably, shifting the objective from state prediction to Onestep Velocity Prediction (c) yields a substantial +14.6  $\mathcal{J} \& \mathcal{F}$  gain. This key result proves that learning a residual (velocity) is a fundamentally more stable and effective task, providing strong initial validation for our flow-based reformulation.

**Effectiveness of Start-Point Focused Adaptations.** Having confirmed the video-to-mask flow as the most promising direction, we dissect our proposed adaptations (rows c-h). The Base Flow model (c), trained with naive uniform sampling, performs poorly at 47.9  $\mathcal{J} \& \mathcal{F}$ , even worse than the one-step velocity predictor. This confirms that a multi-step process is not inherently superior; it

432  
 433  
 434  
 435  
 436  
 437  
 438  
 439  
 440  
 441  
 442  
 443  
 444  
 445  
 446  
 447  
 448  
 449  
 450  
 451  
 452  
 453  
 454  
 455  
 456  
 457  
 458  
 459  
 460  
 461  
 462  
 463  
 464  
 465  
 466  
 467  
 468  
 469  
 470  
 471  
 472  
 473  
 474  
 475  
 476  
 477  
 478  
 479  
 480  
 481  
 482  
 483  
 484  
 485

Table 3: Analysis of VAE adaptation strategies. We measure both the mask reconstruction quality (Recon.) and the resulting performance (Perf.) on the MeViS *valid<sub>u</sub>* set with a fixed flow model. VAE is tuned on MeViS training set.

VAE Adaptation Strategy	Recon. $\mathcal{J} \& \mathcal{F}$	Perf. $\mathcal{J} \& \mathcal{F}$
Frozen VAE	29.7	19.6
Add Trainable Conv Head	85.4	53.2
<b>Finetuning Decoder (ours default)</b>	<b>99.1</b>	<b>60.6</b>

must be correctly stabilized. The introduction of **Boundary-Biased Sampling (BBS)** provides the definitive solution. As shown in rows (d)-(f), forcing the model to focus on the start of the trajectory by oversampling  $t = 0$  almost single-handedly unlocks the potential of the multi-step flow. Even a moderate bias of  $p = 0.25$  (d) brings a massive +7.3 point improvement. The performance peaks at  $p = 0.5$  (e), yielding a total gain of +10.0  $\mathcal{J} \& \mathcal{F}$  over the baseline. While a more extreme bias of  $p = 0.75$  (f) leads to a slight performance drop, the score of 56.5 remains substantially higher than the baseline, demonstrating that the strategy is robust and effective across a reasonable range of hyperparameters. This confirms that mastering the initial, text-guided velocity is the most critical factor for success. Finally, Direct Video Injection (DVI) (h) provides a persistent context anchor throughout the trajectory, preventing drift and adding a significant +2.0  $\mathcal{J} \& \mathcal{F}$ .

**Effectiveness of the T2V Pretrain Model.** Finally, we validate the central premise of our work: leveraging the power of large-scale T2V models. As shown in row (i), training our model from scratch without the pretrained weights (**-WI**) results in a complete performance collapse to 21.1  $\mathcal{J} \& \mathcal{F}$ . This underscores that our contributions are not generic training method, but are specifically designed to effectively harness and adapt the powerful priors learned by generative foundation models for this challenging discriminative task.

**Effectiveness of the VAE Adaptation.** A crucial step in our method is adapting the pretrained VAE to accurately transform between the latent space and the pixel space of binary masks. As shown in Table 3, we evaluate several adaptation strategies. In all experiments, we freeze the VAE encoder to preserve its powerful pretrained features and maintain a stable latent space. We then compare three decoder configurations: keeping it frozen, adding a simple convolutional head, and full-parameter finetuning. The results are definitive: fully finetuning the decoder dramatically improves mask reconstruction quality, which directly translates to a significant boost in final RVOS performance. The The visualization results which we provide in Appendix B also demonstrate the effectiveness of such adaptation.

## 5 CONCLUSION AND FUTURE WORK

In this work, we introduce FlowRVS, a framework that moves beyond using T2V models as mere feature extractors and instead reformulates RVOS as a continuous, text-conditioned flow from video to mask. Our core contribution is demonstrating that this paradigm shift, when combined with our proposed start-point focused adaptations (BBS, SPA, DVI), successfully aligns the generative strengths of T2V models with the discriminative demands of the task, leading to state-of-the-art performance. Our findings validate that the key to unlocking these models lies in principled adaptation, proving that by fortifying the flow’s structured starting point, the philosophical gap between generative processes and discriminative objectives can be effectively bridged.

Looking forward, we believe the paradigm of modeling understanding tasks as conditional deformation processes holds significant potential beyond RVOS. And our insight in stabilizing discriminative, start-point-critical flows provide a crucial blueprint for the future. As even bigger and more powerful foundation models emerge, these techniques will be essential for harnessing their full potential and applying their remarkable capabilities to the vast amount of video understanding tasks.

486 REFERENCES  
487

488 Zechen Bai, Tong He, Haiyang Mei, Pichao Wang, Ziteng Gao, Joya Chen, Zheng Zhang, and  
489 Mike Zheng Shou. One token to seg them all: Language instructed reasoning segmentation in  
490 videos. *Advances in Neural Information Processing Systems*, 37:6833–6859, 2024.

491 Claudia Cuttano, Gabriele Trivigno, Gabriele Rosi, Carlo Masone, and Giuseppe Averta. Samwise:  
492 Infusing wisdom in sam2 for text-driven video segmentation. In *Proceedings of the Computer*  
493 *Vision and Pattern Recognition Conference*, pp. 3395–3405, 2025.

494 Henghui Ding, Chang Liu, Shuting He, Xudong Jiang, and Chen Change Loy. Mevis: A large-scale  
495 benchmark for video segmentation with motion expressions. In *Proceedings of the IEEE/CVF*  
496 *international conference on computer vision*, pp. 2694–2703, 2023.

497 Yu Gao, Haoyuan Guo, Tuyen Hoang, Weilin Huang, Lu Jiang, Fangyuan Kong, Huixia Li, Jiashi Li,  
498 Liang Li, Xiaojie Li, et al. Seedance 1.0: Exploring the boundaries of video generation models.  
499 *arXiv preprint arXiv:2506.09113*, 2025.

500 Kirill Gavrilyuk, Amir Ghodrati, Zhenyang Li, and Cees GM Snoek. Actor and action video seg-  
501 mentation from a sentence. In *Proceedings of the IEEE conference on computer vision and pattern*  
502 *recognition*, pp. 5958–5966, 2018.

503 Ming Gui, Johannes Schusterbauer, Ulrich Prestel, Pingchuan Ma, Dmytro Kotovenko, Olga  
504 Grebenkova, Stefan Andreas Baumann, Vincent Tao Hu, and Björn Ommer. Depthfm: Fast gen-  
505 erative monocular depth estimation with flow matching. In *Proceedings of the AAAI Conference*  
506 *on Artificial Intelligence*, volume 39, pp. 3203–3211, 2025.

507 Shuting He and Henghui Ding. Decoupling static and hierarchical motion perception for referring  
508 video segmentation. In *Proceedings of the IEEE/CVF Conference on Computer Vision and Pattern*  
509 *Recognition*, pp. 13332–13341, 2024.

510 Ronghang Hu, Marcus Rohrbach, and Trevor Darrell. Segmentation from natural language expres-  
511 sions. In *European conference on computer vision*, pp. 108–124. Springer, 2016.

512 Dengyang Jiang, Zanyi Wang, Hengzhuang Li, Sizhe Dang, Teli Ma, Wei Wei, Guang Dai, Lei  
513 Zhang, and Mengmeng Wang. Affordancesam: Segment anything once more in affordance  
514 grounding. *arXiv preprint arXiv:2504.15650*, 2025.

515 Sahar Kazemzadeh, Vicente Ordonez, Mark Matten, and Tamara Berg. Referitgame: Referring to  
516 objects in photographs of natural scenes. In *Proceedings of the 2014 conference on empirical*  
517 *methods in natural language processing (EMNLP)*, pp. 787–798, 2014.

518 Anna Khoreva, Anna Rohrbach, and Bernt Schiele. Video object segmentation with language refer-  
519 ring expressions. In *Asian conference on computer vision*, pp. 123–141. Springer, 2018.

520 Alexander Kirillov, Eric Mintun, Nikhila Ravi, Hanzi Mao, Chloe Rolland, Laura Gustafson, Tete  
521 Xiao, Spencer Whitehead, Alexander C Berg, Wan-Yen Lo, et al. Segment anything. In *Proceed-  
522 ings of the IEEE/CVF international conference on computer vision*, pp. 4015–4026, 2023.

523 Xin Lai, Zhuotao Tian, Yukang Chen, Yanwei Li, Yuhui Yuan, Shu Liu, and Jiaya Jia. Lisa: Rea-  
524 soning segmentation via large language model. In *Proceedings of the IEEE/CVF Conference on*  
525 *Computer Vision and Pattern Recognition*, pp. 9579–9589, 2024.

526 Gen Li, Varun Jampani, Deqing Sun, and Laura Sevilla-Lara. Locate: Localize and transfer object  
527 parts for weakly supervised affordance grounding. In *Proceedings of the IEEE/CVF Conference*  
528 *on Computer Vision and Pattern Recognition*, pp. 10922–10931, 2023.

529 Tianming Liang, Haichao Jiang, Wei-Shi Zheng, and Jian-Fang Hu. Referdino-plus: 2nd solution  
530 for 4th puvw mevis challenge at cvpr 2025. *arXiv preprint arXiv:2503.23509*, 2025a.

531 Tianming Liang, Kun-Yu Lin, Chaolei Tan, Jianguo Zhang, Wei-Shi Zheng, and Jian-Fang Hu.  
532 Referdino: Referring video object segmentation with visual grounding foundations. *arXiv*  
533 *preprint arXiv:2501.14607*, 2025b.

540 Lang Lin, Xueyang Yu, Ziqi Pang, and Yu-Xiong Wang. Glus: Global-local reasoning unified into a  
 541 single large language model for video segmentation. In *Proceedings of the Computer Vision and*  
 542 *Pattern Recognition Conference*, pp. 8658–8667, 2025.

543 Yaron Lipman, Ricky TQ Chen, Heli Ben-Hamu, Maximilian Nickel, and Matt Le. Flow matching  
 544 for generative modeling. *arXiv preprint arXiv:2210.02747*, 2022.

545 Haotian Liu, Chunyuan Li, Qingyang Wu, and Yong Jae Lee. Visual instruction tuning. *Advances*  
 546 *in neural information processing systems*, 36:34892–34916, 2023.

547 Xingchao Liu, Chengyue Gong, and Qiang Liu. Flow straight and fast: Learning to generate and  
 548 transfer data with rectified flow. *arXiv preprint arXiv:2209.03003*, 2022.

549 Yixin Liu, Kai Zhang, Yuan Li, Zhiling Yan, Chujie Gao, Ruoxi Chen, Zhengqing Yuan, Yue Huang,  
 550 Hanchi Sun, Jianfeng Gao, et al. Sora: A review on background, technology, limitations, and  
 551 opportunities of large vision models. *arXiv preprint arXiv:2402.17177*, 2024.

552 Zhuoyan Luo, Yicheng Xiao, Yong Liu, Shuyan Li, Yitong Wang, Yansong Tang, Xiu Li, and Yujiu  
 553 Yang. Soc: Semantic-assisted object cluster for referring video object segmentation. *Advances in*  
 554 *Neural Information Processing Systems*, 36:26425–26437, 2023.

555 Feiyu Pan, Hao Fang, Fangkai Li, Yanyu Xu, Yawei Li, Luca Benini, and Xiankai Lu. Semantic and  
 556 sequential alignment for referring video object segmentation. In *Proceedings of the Computer*  
 557 *Vision and Pattern Recognition Conference*, pp. 19067–19076, 2025.

558 Tianhe Ren, Shilong Liu, Ailing Zeng, Jing Lin, Kunchang Li, He Cao, Jiayu Chen, Xinyu Huang,  
 559 Yukang Chen, Feng Yan, et al. Grounded sam: Assembling open-world models for diverse visual  
 560 tasks. *arXiv preprint arXiv:2401.14159*, 2024.

561 Robin Rombach, Andreas Blattmann, Dominik Lorenz, Patrick Esser, and Björn Ommer. High-  
 562 resolution image synthesis with latent diffusion models. In *Proceedings of the IEEE/CVF confer-*  
 563 *ence on computer vision and pattern recognition*, pp. 10684–10695, 2022.

564 Team Wan, Ang Wang, Baole Ai, Bin Wen, Chaojie Mao, Chen-Wei Xie, Di Chen, Feiwu Yu,  
 565 Haiming Zhao, Jianxiao Yang, et al. Wan: Open and advanced large-scale video generative  
 566 models. *arXiv preprint arXiv:2503.20314*, 2025.

567 Dongming Wu, Tiancai Wang, Yuang Zhang, Xiangyu Zhang, and Jianbing Shen. Onlinerefer: A  
 568 simple online baseline for referring video object segmentation. In *Proceedings of the IEEE/CVF*  
 569 *International Conference on Computer Vision*, pp. 2761–2770, 2023.

570 Jiannan Wu, Yi Jiang, Peize Sun, Zehuan Yuan, and Ping Luo. Language as queries for referring  
 571 video object segmentation. In *Proceedings of the IEEE/CVF Conference on Computer Vision and*  
 572 *Pattern Recognition*, pp. 4974–4984, 2022.

573 Ning Xu, Linjie Yang, Yuchen Fan, Jianchao Yang, Dingcheng Yue, Yuchen Liang, Brian Price,  
 574 Scott Cohen, and Thomas Huang. Youtube-vos: Sequence-to-sequence video object segmen-  
 575 tation. In *Proceedings of the European conference on computer vision (ECCV)*, pp. 585–601, 2018.

576 Cilin Yan, Haochen Wang, Shilin Yan, Xiaolong Jiang, Yao Hu, Guoliang Kang, Weidi Xie, and  
 577 Efratios Gavves. Visa: Reasoning video object segmentation via large language models. In  
 578 *European Conference on Computer Vision*, pp. 98–115. Springer, 2024a.

579 Shilin Yan, Renrui Zhang, Ziyu Guo, Wenchao Chen, Wei Zhang, Hongyang Li, Yu Qiao, Hao Dong,  
 580 Zhongjiang He, and Peng Gao. Referred by multi-modality: A unified temporal transformer for  
 581 video object segmentation. In *Proceedings of the AAAI Conference on Artificial Intelligence*,  
 582 volume 38, pp. 6449–6457, 2024b.

583 Licheng Yu, Patrick Poirson, Shan Yang, Alexander C Berg, and Tamara L Berg. Modeling context  
 584 in referring expressions. In *European conference on computer vision*, pp. 69–85. Springer, 2016.

585 Lvmin Zhang, Anyi Rao, and Maneesh Agrawala. Adding conditional control to text-to-image  
 586 diffusion models. In *Proceedings of the IEEE/CVF international conference on computer vision*,  
 587 pp. 3836–3847, 2023.

594 Ruixin Zhang, Jiaqing Fan, Yifan Liao, Qian Qiao, and Fanzhang Li. Temporal-conditional re-  
595 ferring video object segmentation with noise-free text-to-video diffusion model. *arXiv preprint*  
596 *arXiv:2508.13584*, 2025.

597 Xizhou Zhu, Weijie Su, Lewei Lu, Bin Li, Xiaogang Wang, and Jifeng Dai. Deformable detr:  
598 Deformable transformers for end-to-end object detection. *arXiv preprint arXiv:2010.04159*, 2020.

599 600 Zixin Zhu, Xuelu Feng, Dongdong Chen, Junsong Yuan, Chunming Qiao, and Gang Hua. Exploring  
601 pre-trained text-to-video diffusion models for referring video object segmentation. In *European*  
602 *Conference on Computer Vision*, pp. 452–469. Springer, 2024.

603  
604  
605  
606  
607  
608  
609  
610  
611  
612  
613  
614  
615  
616  
617  
618  
619  
620  
621  
622  
623  
624  
625  
626  
627  
628  
629  
630  
631  
632  
633  
634  
635  
636  
637  
638  
639  
640  
641  
642  
643  
644  
645  
646  
647

648  
649

## APPENDIX

650  
651

## A HYPERPARAMETERS SETTINGS

652  
653  
654

All our models are trained using the AdamW optimizer. We detail the key hyperparameters for our main experiments on Ref-YouTube-VOS and MeViS in Table 4.

655  
656  
657

Table 4: Key hyperparameters for the training of FlowRVS. We detail the settings for the 2D pre-training, the main DiT fine-tuning on video datasets, and the separate VAE decoder adaptation.

Hyperparameter	2D Pre-training (RefCOCO+g)	Video DiT Fine-tuning (Ref-YT-VOS & MeViS)	VAE Decoder Fine-tuning (on MeViS)
<i>Optimizer Configuration</i>			
Optimizer	AdamW	AdamW	AdamW
Peak Learning Rate	7e-5	6e-5	8e-5
LR Schedule	None	None	None
Warmup Steps	0	0	0
Weight Decay	5e-4	5e-4	5e-4
Adam $\beta_1, \beta_2$	(0.9, 0.999)	(0.9, 0.999)	(0.9, 0.999)
<i>Training Schedule &amp; Loss</i>			
Total Training Epochs	6	7 / 6	1
Global Batch Size	8	8	4
Per-GPU Batch Size	1	1	1
Gradient Accumulation Steps	1	1	1
Mixed Precision	bfloat16	bfloat16	bfloat16
Loss Function	L2 (MSE Loss)	L2 (MSE Loss)	Combined Focal + Dice Loss ( $\alpha = 0.25, \gamma = 2.0$ )

666

## B VAE RECONSTRUCTION COMPARISON

667  
668  
669  
670  
671  
672

As shown in Table 3 and below Figure 5. The vanilla VAE fails to reconstruct accurate masks, a discrepancy we attribute to the extreme domain shift between mask images (binary 0/1) and the natural-photo distribution on which the decoder was pre-trained. Fine-tuning the decoder resolves this failure, indicating that the frozen encoder already encodes sufficient mask-related structure and that only the decoder needs to adapt to the new visual modality.

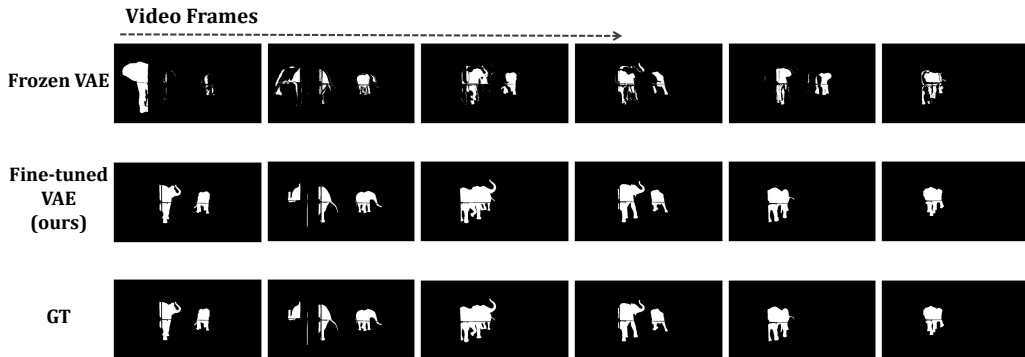


Figure 5: Visualization of VAE reconstruction results

694  
695  
696

## C MORE QUALITATIVE RESULTS

697  
698  
699  
700  
701

In this section, we provide additional qualitative results of FlowRVS on challenging video-text pairs. These examples further demonstrate that our holistic, flow-based approach successfully handles complex language and dynamic scenes, particularly in scenarios involving significant occlusion and nuanced textual descriptions.

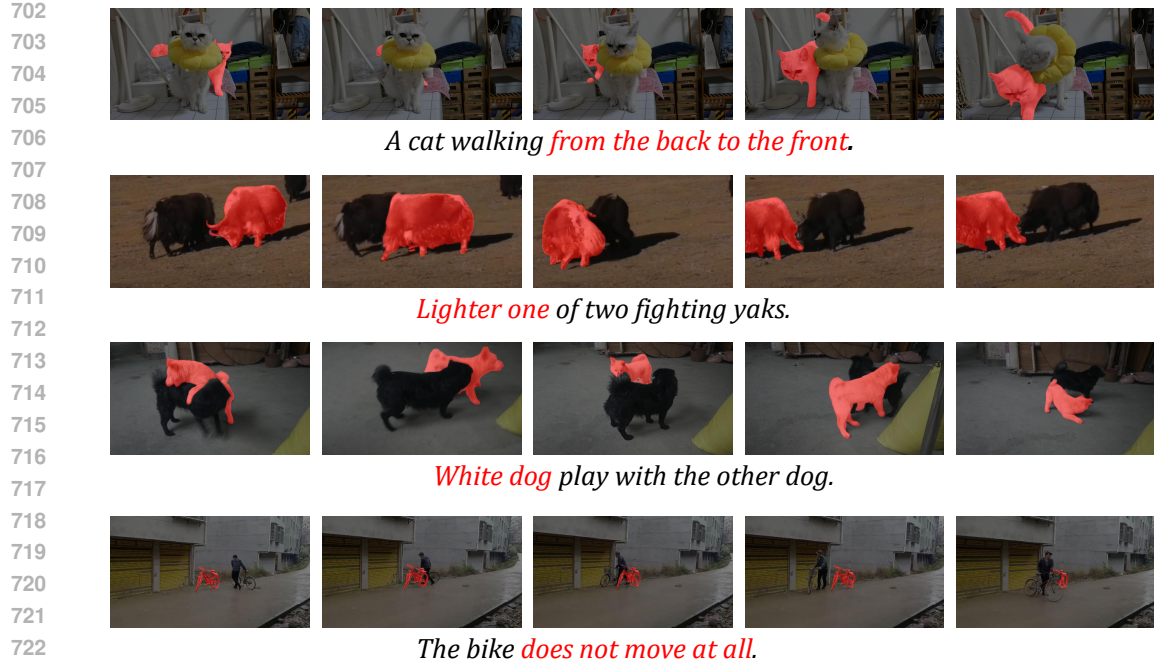


Figure 6: visualization example of FlowRVS results on MeViS-Valid-u.

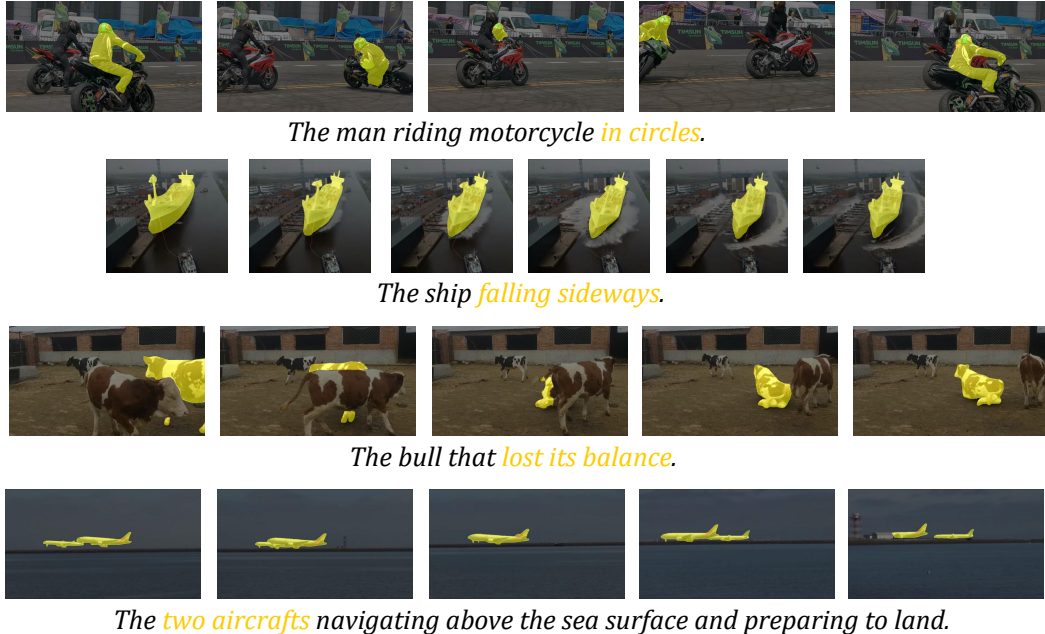


Figure 7: visualization example of FlowRVS results on MeViS-Valid.

## D COMPREHENSIVE RESULTS

752 While our method demonstrates strong performance, it is not without limitations. We present two  
 753 typical failure modes on Figure 9. For complex relational phrases requiring fine-grained interaction  
 754 understanding, such as "swings its tail and strikes the head" on the top row, the model correctly iden-  
 755 tifies the primary subject (the horse) but fails to isolate the specific horse performing the action. This  
 suggests a limitation in comprehending intricate multi-part actions. In scenarios with multiple sim-

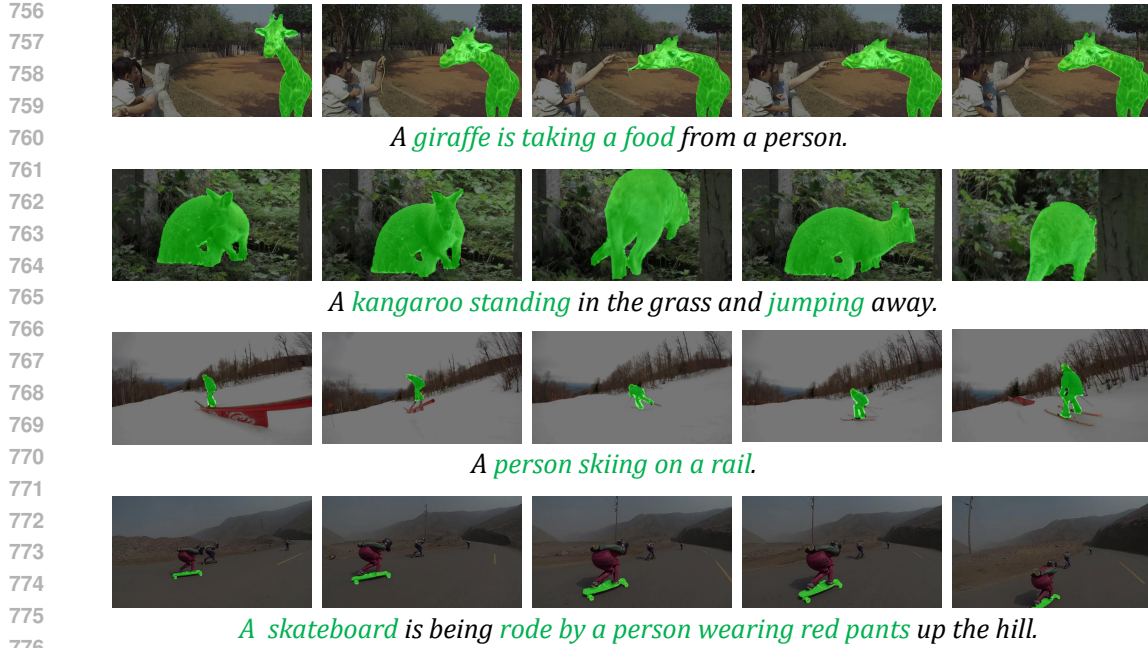


Figure 8: visualization example of FlowRVS results on Ref-YouTube-VOS-Valid.

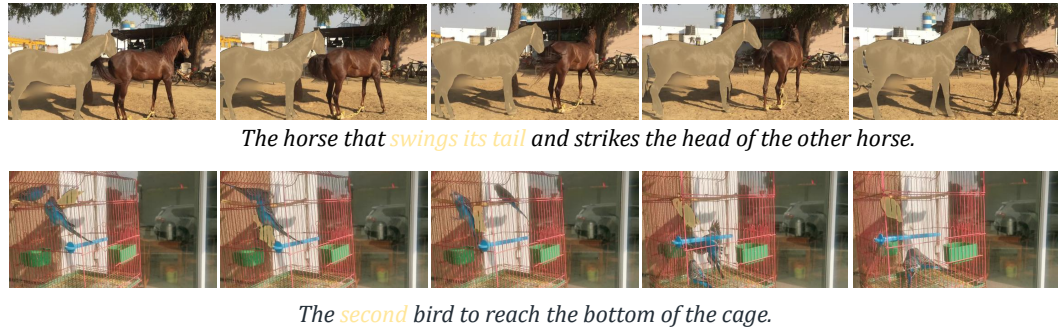


Figure 9: failure cases of FlowRVS results.

793 ilar objects and temporal ordering cues ("the second bird") on the bottom row, the model struggles  
794 to accurately resolve the ambiguity. It incorrectly segments the first bird that moves, indicating that  
795 while our temporal modeling is strong, it can be confounded by challenging counting and ordering  
796 logic within dense scenes.

797 To address the question of generalization to unseen actions and challenging description, we tested  
798 our model on phrases not present in the training data, such as "the dog somersaulting." As shown  
799 on Figure 10, FlowRVS successfully identifies and segments the dog throughout its complex, non-  
800 rigid motion. This demonstrates that our method does not merely memorize action-object pairings  
801 from the training set. Instead, by leveraging the rich spatio-temporal and semantic priors from the  
802 pretrained T2V model, it develops a more fundamental understanding based on open-set vocabulary  
803 queries that allows it to generalize to novel and dynamic actions.

## E DETAILS ABOUT PROPOSED IMPROVEMENTS

### E.1 BOUNDARY-BIASED SAMPLING (BBS)

804  
805  
806  
807  
808  
809 BBS is a training strategy to emphasize the crucial initial step of the flow ( $t = 0$ ). Formally, we  
sample the timestep  $t$  from a mixed probability distribution, whose probability density function  $f(t)$



The dog somersaulting.

Figure 10: novel action phrases out of MeViS training.

is defined as:  $f(t) = p \cdot \delta(t) + (1 - p) \cdot \mathcal{U}(t|0, 1)$  where  $\delta(t)$  is the Dirac delta function representing a point mass at  $t = 0$ ,  $\mathcal{U}(t|0, 1)$  is the uniform distribution on the interval  $[0, 1]$ , and  $p$  is the bias probability. In practice, this means we sample  $t = 0$  with probability ( $p=0.5$ ).

## E.2 START-POINT AUGMENTATION (SPA)

SPA is a crucial regularizer to improve the robustness of our convergent (video-to-mask) flow. For a given video  $V$ , the VAE encoder  $E_\phi$  predicts a posterior distribution  $q(z|V) = \mathcal{N}(z|\mu_V, \sigma_V^2)$ , where  $\mu_V$  and  $\sigma_V^2$  are directly inherited from the VAE. Instead of using the deterministic mean  $\mu_V$ , SPA samples the starting point  $z'_0$  from this posterior:  $z'_0 \sim \mathcal{N}(z|\mu_V, \sigma_V^2)$ . This sampled latent  $z'_0$  is then normalized before being used the ODE solver. By augmenting the training data with samples from the local neighborhood of each video's true latent representation, SPA forces the model to learn a smoother and more generalizable velocity field.

## E.3 DIRECT VIDEO INJECTION (DVI)

DVI provides the model with a persistent anchor to the original video content throughout the ODE trajectory. It is implemented by concatenating the current state  $z_t$  with the initial video latent  $z_0$ . This changes the input tensor's shape from  $[B, C, T, H, W]$  to  $[B, 2 * C, T, H, W]$ . This is handled by modifying the first convolutional layer of the DiT to accept  $2 * C$  input channels, while all subsequent layers remain unchanged.